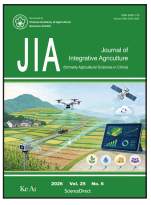
Journal of Integrative Agriculture 2026, 25(6): 2569–2579

Available online at ScienceDirect

Journal of Integrative Agriculture



RESEARCH ARTICLE

Adaptability of plants to phosphorus deficiency shapes bacterial community and spatial patterns of enzyme activities in rhizosphere

Xiaomin Ma[1*], Lisha Zeng[1*], Jialin Wang[1], Yan Zhou[1], Yongjian Zhang[1, 2], Junhui Chen[1#], Yakov Kuzyakov[3, 4]

[1] *Key Laboratory of Soil Remediation and Quality Improvement of Zhejiang Province, Zhejiang A&F University, Hangzhou 311300, China*
[2] *College of Optical, Mechanical, and Electrical Engineering, Zhejiang A&F University, Hangzhou 311300, China*
[3] *Department of Soil Science of Temperate Ecosystems/Department of Agricultural Soil Science, University of Göttingen, Göttingen 37077, Germany*
[4] *Peoples Friendship University of Russia (RUDN University), Moscow 117198, Russia*

Highlights

- Lupine exhibited enhanced Phosphorus (P) deficiency adaptation through increased root exudation compared to maize.
- Low P conditions inhibited maize growth but enhanced root exudation efficiency compared to high P conditions.
- Enhanced root exudation promoted r-strategists while reducing K-strategists.
- Maize demonstrated increased enzyme activities and hotspot areas correlating with K-strategist abundance.
- Both plant and microbial factors influenced enzyme activity and hotspot area distribution.

Abstract

Phosphorus (P) availability influences the spatial distribution of carbon (C)-cycling enzyme activities in the rhizosphere through its effects on plant growth and microbial activity. However, the influence of P availability on the spatial patterns of C and P hydrolase activities remains unclear in the rhizosphere of Maize (*Zea mays* L.) and narrow-leaf lupine (*Lupinus angustifolius* L.), which exhibit contrasting P deficiency adaptation and acquisition strategies. This study analyzed the spatial patterns of C and P hydrolase activities through zymography and correlated them with bacterial community structure in maize and lupine rhizospheres. Under P-deficient conditions, maize exhibited severe growth restriction while demonstrating a 2.2–9.6-fold increase in root exudation compared to P-sufficient conditions. The enhanced exudation under P deficiency promoted r-strategist bacterial proliferation (e.g., Ktedonobacteria and Xanthomonadales) while reducing K-strategist abundance (Actinobacteriota, Chloroflexia, and Alphaproteobacteria). Maize rhizosphere enzyme activities and hotspot areas demonstrated positive correlation with K-strategist abundance and negative correlation with r-strategist abundance. P-sufficient maize exhibited 15–550% higher C- and P-cycle-related enzyme activity and hotspot areas, attributed to its enhanced root system and predominance of K-strategists with superior enzyme synthesis capabilities. Lupine demonstrated superior P deficiency adaptation, producing 2–19 times more DOC and organic acids than maize. Consequently, lupine showed no significant alterations in enzyme activity, hotspot areas, or bacterial community composition in response to P availability. These findings demonstrate that plant-specific P deficiency adaptation mechanisms distinctly influence the spatial distribution of C-cycling enzyme activity and bacterial community structure in the rhizosphere.

Keywords: phosphorus acquisition strategy, soil zymography, microbial strategies, root exudate, hotspot areas

1. Introduction

Phosphorus (P) deficiency significantly limits plant development in both natural ecosystems and agricultural systems (Cong *et al.* 2020). This limitation occurs because P is frequently bound in organic forms or exists as insoluble iron, aluminum, and calcium phosphates. These conditions result in low bioavailability and restricted mobility in most agricultural soils globally (Ma *et al.* 2021d; Lambers

Received 8 April 2025; Received in revised form 5 June 2025; Accepted 25 June 2025; Available online 21 August 2025
Xiaomin Ma, Mobile: +86-15855363948, E-mail: maxiaomin@zafu.edu.cn; #Correspondence Junhui Chen, Mobile: +86-13906814189, E-mail: junhui@zafu.edu.cn
* These authors contributed equally to this study.

© 2026 CAAS. Publishing services by Elsevier B.V. on behalf of KeAi Communications Co. Ltd. This is an open access article under the CC BY-NC-ND license (http://creativecommons.org/licenses/by-nc-nd/4.0/). Peer review under responsibility of Editorial Board of *Journal of Integrative Agriculture*.
doi: 10.1016/j.jia.2025.08.017

2022; Jiang *et al*. 2025). Plants have evolved various adaptive strategies to optimize P assimilation under low soil P conditions. These strategies include modifying root architecture through increased root branching, elongation, and hair density to enhance soil exploration capacity (Postma *et al.* 2014; Ma *et al.* 2019). Plants also make physiological adjustments, including the secretion of carboxylates, phosphatases, and protons, to facilitate the solubilization and hydrolysis of fixed P (Hinsinger 2001; Pang *et al.* 2018; Chen *et al.* 2024). Moreover, plant associations with microorganisms, particularly symbiosis with arbuscular mycorrhizal fungi (AMF), expand the exploited soil area and enable phosphate-solubilizing bacteria to release fixed P (Zhang *et al.* 2016; Ma *et al.* 2021b).

Phosphorus availability affects the spatial distribution of C-cycling enzyme activities in the rhizosphere due to the interconnected relationship between C and P cycles (Soong *et al.* 2018; Ma *et al.* 2023). While P availability directly influences plant growth, root-secreted enzymes associated with the C cycle indirectly regulate C allocation to belowground biomass. This allocation process subsequently shapes microbial community structure and function, thereby modulating enzyme activities in the rhizosphere (Philippot *et al.* 2013; Hao *et al.* 2022).

The distribution and activity of enzymes in the rhizosphere emerge from complex interactions between plants and microbial communities (Zhang *et al*. 2021). A well-developed root system with adequate P availability promotes plant growth and facilitates the formation of rhizosphere hotspots. However, under high P conditions, the allocation of photosynthates to belowground biomass decreases (Hammond and White 2008). Consequently, rhizosphere microorganisms, experiencing C limitation, produce more enzymes to hydrolyze soil organic matter (Ma *et al.* 2021a). Conversely, P deficiency may result in decreased enzyme activities and reduced hotspot areas.

Plant P acquisition strategies regulate the spatial distribution of roots and C-related enzyme activities in the rhizosphere. Root morphology determines the location of root-derived C, thereby influencing the spatial distribution of enzymes produced by both roots and microorganisms (Neumann and Martinoia 2002; Bardgett *et al*. 2014). Root physiological traits influence the quality and quantity of exudates, which affect microbial access to C sources and alter the composition of the rhizosphere microbial community (Walker *et al.* 2003; Wang and Kuzyakov 2024). Enhanced root exudation stimulates the proliferation of r-strategist bacteria, which demonstrate lower carbon use efficiency and reduced enzyme synthesis rates compared to K-strategist microorganisms (Fang *et al.* 2018; Li *et al.* 2024). Additionally, AMF affect the spatial distribution of enzyme activities within the rhizosphere and mycorrhizosphere by utilizing up to 20% of the total C photosynthesized by plants (Frey 2019; Parihar *et al.* 2020).

Plants have developed diverse adaptations to manage P deficiency. Lupine and maize demonstrate distinct adaptation and acquisition strategies under P limitation. Lupine, a leguminous species, exhibits P efficiency and adapts to low P conditions through the release of carboxylic acids and acid phosphatases to mobilize soil P. In contrast, maize, a gramineous species that depends on root morphological modifications and mycorrhizal symbiosis, shows greater susceptibility to P deficiency (Zhang *et al.* 2016; Wen *et al.* 2019). Several critical questions regarding P availability's effects on the spatial distribution and *in situ* activity of C-cycle enzymes require investigation: 1) How do the distinct adaptation strategies of lupine and maize under P deficiency affect plant growth, root exudation, and the spatial distribution of C-related enzyme activities? 2) How do lupine and maize modify their nutrient acquisition strategies in response to P availability, and how does this influence the structure and function of the rhizosphere bacterial community? 3) What is the relationship between bacterial community composition and the spatial distribution of enzyme activities? Although AMF serve an essential role in C and P translocation within the rhizosphere, this study emphasizes the bacterial community since AMF possess limited direct capability to produce extracellular enzymes and typically collaborate with other bacteria (Choreño-Parra and Treseder 2024).

To investigate these questions, lupine and maize were cultivated under low and high P conditions. The potential activities and spatial distributions of acid phosphatase, cellobiohydrolase, and β-N-acetylglucosaminidase in the rhizosphere were evaluated using zymography. The composition of the rhizosphere bacterial community and interactions among taxa were analyzed through high-throughput sequencing of 16S rRNA genes and co-occurrence network analysis. Furthermore, plant growth, root exudate content (dissolved organic carbon (DOC) and carboxylic acids), and mycorrhizal colonization ratio were determined. We hypothesized that: 1) Maize would demonstrate higher susceptibility to P deficiency, showing stronger responses in plant growth and root exudation, leading to greater effects on the spatial distribution of C-related enzyme activity compared to lupine; 2) plants grown in low-P soil would alter the rhizosphere bacterial community toward r-strategists due to increased root exudation, with this change being more evident in maize than in lupine; 3) enzyme activities and hotspot areas would increase with the abundance of microbial K-strategists but decrease with the abundance of microbial r-strategists.

2. Materials and methods

2.1. Soil and plant preparation

Soil with low P content was obtained from the top 20 cm of a forest in Lin'an, Hangzhou City, Zhejiang Province, China. Based on the Food and Agriculture Organization of the United Nations (FAO) soil classification system (WRB 2006), the soil was categorized as Ferrasol. The soil exhibited a pH of 5.21, available nitrogen (N) content of 51 mg kg^{-1}, total P of 288 mg kg^{-1}, available P of 2.6 mg kg^{-1}, available potassium (K) of 193 mg kg^{-1}, and organic C content of 2.85%. The air-dried soil was filtered through a 2 mm mesh and combined with quartz sand (0.5–2 mm in diameter) at a 7:3 ratio (soil:sand).

Soluble fertilizers were incorporated into the soil-sand mixture at the following concentrations (mg kg^{-1}): 200 N as urea, 100 K as K_2SO_4, 100 Mg as $MgSO_4$, 2 Fe

as $FeSO_4 \cdot 7H_2O$, 1 Cu as $CuSO_4 \cdot 5H_2O$, and 2.6 Zn as $ZnSO_4 \cdot 7H_2O$. Two P application treatments were established: 32 and 140 mg P kg^{-1} in the form of Na_3PO_4, representing low and high P conditions, respectively (Wang L *et al.* 2021). The Olsen-P of uniformly nutrient-treated soil after fertilization measured 4.2 mg kg^{-1} for low P and 12.8 mg kg^{-1} for high P treatments. Each rhizobox (35 cm×18 cm×2 cm) contained approximately 1.5 kg of the soil-sand mixture.

Seeds of maize (*Zea mays* L.) and narrow-leaf lupine (*Lupinus angustifolius* L.) underwent sterilization in a 10% hydrogen peroxide (H_2O_2) solution for 30 min and germinated for three days. Subsequently, one maize seedling or two narrow-leaf lupine seedlings were transplanted into each rhizobox at a depth of 1 cm. The experiment was conducted in a greenhouse during the summer of 2023. Each treatment comprised six replicates, yielding a total of 24 rhizoboxes (6 replicates×2 treatments×2 plant species). During the growth period, rhizoboxes were positioned at a 45° angle to facilitate root growth along the lower edges of the Plexiglas covers. To maintain uniform soil moisture levels, rhizoboxes were weighed and irrigated daily to sustain soil moisture at 50–60% of the water-holding capacity.

2.2. *In situ* soil zymography and imaging

After six weeks of plant growth, soil zymography was implemented to visualize the spatial distribution of enzyme activities. The fluorogenic substrates 4-methylumbelliferyl (MUF)-phosphate, 4-MUF-β-D-cellobioside, and 4-MUF-N-acetyl-β-D-glucosaminide were utilized to detect acid phosphatase (ACP), cellobiohydrolase (Cello), and β-N-acetylglucosaminidase (NAG) activities, respectively. Each substrate was dissolved in an acetic acid buffer (pH=5.0) to achieve a final concentration of 0.5 mmol L^{-1}. A polyamide membrane with a pore size of 0.45 μm (Haining Yichun Analytical Instrument Co., Ltd., Taoyuan Brand, China) was saturated with the substrate solution and attached to the surface of each rhizobox, ensuring contact with plant roots. The membrane remained in contact for 1 h. After incubation, the membranes were carefully removed from the soil surface, and any adhering soil particles were gently cleared. The membranes were then exposed to UV light (excitation wavelength: 355 nm) in a darkened room and photographed using a camera with standardized settings. The imaging setup, including the camera (Z 7II, Nikon Corporation, Japan), the UV light source, and the sample position, remained constant throughout the process. A calibration line was established following the method described by Ma *et al.* (2018).

Image processing and analysis were performed using the open-source software Fiji (https://imagej.net/software/fiji/downloads). Zymogram images were converted into 8-bit grayscale values and transformed into enzyme activity data through linear regression analysis. To determine bulk soil enzyme activity, at least five rectangular regions, each situated at least 1 cm away from the root, were selected. The spatial distribution of rhizosphere enzyme activity was assessed by drawing five randomly selected lines, each 50 pixels wide, across the roots of each plant. The rhizosphere extent was calculated as the distance from the root center to the nearest point where enzyme activity exceeded that of the bulk soil. The mean enzyme activity within the rhizosphere was determined through zymogram segmentation. Areas where enzyme activity exceeded the average rhizosphere activity were designated as hotspots, and their sizes were calculated based on pixel dimensions.

2.3. Soil and plant sampling and analysis

Following soil zymography, the plants were carefully extracted from the rhizoboxes. The roots were gently shaken to remove loosely attached soil, while the soil remaining adhered to the roots was designated as rhizosphere soil. Each rhizosphere soil sample was divided into two subsamples: one for enzyme activity analysis, stored at –20°C, and one for bacterial community composition analysis, preserved at –80°C. The roots of each plant were thoroughly cleaned with water and then submerged in deionized water for 2 h to collect root exudates. Subsequently, the plant shoots were removed, and the roots were scanned using a flatbed scanner (Epson Expression 1000 XL, Tokyo, Japan). The scanned images were analyzed using WinRHIZO software (Regent Instruments, Canada) to assess root morphology. Roots still attached to the shoots and detached roots were scanned and analyzed separately. To determine biomass, the shoots and roots were dried at 60°C for 3 days, after which their dry weights were recorded. Shoot P content was extracted *via* pressure digestion in concentrated nitric acid and quantified using inductively coupled plasma optical emission spectroscopy (ICP-OES) (Spectro Analytical Instruments, Kleve, Germany).

2.4. Root exudate and mycorrhizal colonization

For root exudate collection, roots were immersed in aerated 50 mL deionized water for 2 h. The resulting exudate solution was filtered through a 0.45 μm pore size membrane and stored at –20°C for subsequent analysis. The dissolved organic carbon (DOC) concentration in the root exudates was determined using a multi-3100 N/C TOC analyzer (Analytik Jena, Germany). The root exudates were analyzed using reversed-phase high-performance liquid chromatography (HPLC) to identify various organic acids, including oxalate, malic acid, citric acid, acetic acid, and others (for a detailed list, see Appendix A). This analysis followed the methodology described by Ma *et al.* (2021b).

Maize root segments within 10 cm from the root tips were cut into approximately 1 cm lengths. These segments underwent treatment with a 10% KOH solution at 90°C for 1 h for clearing, followed by staining with a 5% ink–acetic acid solution (Vierheilig *et al.* 1998). For each replicate, 30 root pieces were randomly selected to evaluate and quantify AMF colonization, following the method described by Trouvelot *et al.* (1986).

2.5. Enzyme activity in the rhizosphere

The activities of ACP, β-Glu, NAG, and Cello were measured using MUF substrates. Suspensions were prepared by combining 1 g of rhizosphere soil with 100 mL of 50 mmol L^{-1} acetate buffer (pH 5.0), followed by shaking for 30 min.

The fluorescent substrates were dissolved in deionized water to achieve a concentration of 200 μmol L^{-1}. In 96-well microplates, 50 μL of soil suspension, 50 μL of buffer, and 100 μL of substrate solution were combined per well. The plates were incubated in the dark at 25°C for 4 h, after which fluorescence was measured using a microplate fluorometer. The excitation wavelength was set to 365 nm, and emission was detected at 450 nm. Enzyme activities were quantified by measuring the release of MUF (nmol h^{-1} g^{-1} dry soil), based on the calibration curve.

2.6. DNA extraction, amplicon sequencing, and bioinformatic analysis

DNA extraction was performed on approximately 0.5 g of fresh rhizosphere soil using the Fast® DNA SPIN Soil DNA Isolation Kit (MP Biomedicals, Santa Ana, CA, USA), according to the manufacturer's protocol. DNA concentration and quality were evaluated using a NanoDrop 2000 UV-Vis spectrophotometer (Thermo Scientific, Wilmington, DE, USA). The bacterial 16S rRNA gene was amplified using barcode-tagged primers 515F/907R. Each sample underwent triplicate amplification in a 20 μL reaction mixture under the following thermal cycling conditions: 27 cycles of denaturation at 95°C for 30 s, annealing at 55°C for 30 s, and extension at 72°C for 45 s, followed by a final extension at 72°C for 10 min. PCR products were separated on 2% agarose gels and purified with the PCR Clean-Up Kit (Yuhua Biomedical Technology Company, Shanghai, China) following the manufacturer's instructions. Purified products were quantified using a Qubit 4.0 (Thermo Fisher Scientific, USA), then pooled in equimolar ratios and sequenced on the Illumina MiSeq platform (Illumina, San Diego, CA, USA) with 300-bp paired-end sequencing, performed by Majorbio Bio-Pharm Technology Co., Ltd. (Shanghai, China). The raw sequencing data were submitted to the NCBI Sequence Read Archive (SRA) database under accession number: PRJNA1152942. Operational taxonomic units (OTUs) were clustered at 97% similarity using UPARSE v. 11 (http://www.drive5.com/uparse/) (Edgar 2013). All bacterial OTU tables were randomly rarefied based on the lowest read count, yielding 42,383 sequences per sample for downstream analysis.

2.7. Statistical analysis

The homogeneity and normality of variance for root and shoot dry weight, total root length, total root surface area, P content, root exudate TOC and organic acids, rhizosphere soil enzyme activity, *in situ* enzyme activity, rhizosphere extent, hotspot areas, and mycorrhizal colonization were evaluated using Levene's test and the Shapiro-Wilk test. Statistical differences in the means of these variables in response to P treatment were analyzed using *t*-tests or one-way ANOVA in SPSS v. 23 software, with significance set at $P<0.05$. Differences in the means of these variables in response to P treatment and plant species were analyzed using two-way ANOVA in SPSS v. 23 software.

To investigate the taxonomic groups responsible for differences in bacterial communities in response to P treatment, linear discriminant analysis effect size (LEfSe) combined with linear discriminant analysis (LDA) was implemented. A logarithmic LDA score threshold of 4.0 was established for identifying discriminative features (Segata *et al*. 2011). The bacterial communities were categorized as r or K strategists based on previous studies (Ling *et al.* 2022; Shang *et al.* 2023). A network was constructed using Spearman correlation scores ($r>0.8$ or $r<-0.8$; $P<0.05$) through Co-occurrence Network inference (CoNet) in Cytoscape v. 3.10.2 (https://cytoscape.software.informer.com/) (Faust and Raes 2012). The network construction included only OTUs with ≥10 reads in at least 3 samples. Network topologies, including nodes, edges, and modularity classes, were analyzed using Gephi v. 0.10.0 (https://gephi.org/) software (Bastian *et al.* 2009).

3. Results

3.1. Effects of P availability on plant growth and root exudates

Independent of P availability, lupine exhibited significantly higher organic acids and DOC content per root biomass, exceeding maize by 2–19 times ($P<0.05$). The organic acids ranged from 2.8–557 μg g^{-1} for lupine compared to 0.03–36.1 μg g^{-1} for maize, while the DOC content ranged from 23–29 mg g^{-1} for lupine compared to 4–13 mg g^{-1} for maize (Fig. 1; Appendix A). Maize grown in high P soil demonstrated 1.6–5.2 times greater root dry weight (0.7 g *vs*. 0.13 g), shoot dry weight (2.2 g *vs*. 0.95 g), total root length (47.8 cm *vs*. 9.2 cm), total root surface area (489 cm^2 *vs*. 117 cm^2), and shoot P content (2.5 mg g^{-1} *vs*. 1.5 mg g^{-1}) compared to those in low P conditions ($P<0.05$) (Fig. 1-A–G). Conversely, maize under low P conditions showed 2.2–9.6 times higher DOC (4.2 mg g^{-1} *vs*.13.8 mg g^{-1}), organic acid contents per root biomass (0.14–36.2 μg g^{-1} *vs*. 0.03–9.7 μg g^{-1}), and mycorrhizal colonization (21% *vs*. 62%) compared to high P conditions ($P<0.05$) (Fig. 1-G and H; Appendix A). Lupine showed no significant response to P availability for these parameters (Fig. 1; Appendix A).

3.2. Rhizosphere enzyme activities, extent of the rhizosphere, and areas of enzyme hotspots inresponse to P availability

The activities of ACP, Glu, Cello, and NAG in the rhizosphere of maize cultivated in high P soil exceeded those in low P soil by 15–31%, with values ranging from 853 to 6,259 μmol g^{-1} h^{-1} in high P soil compared to 699 to 5,463 μmol g^{-1} h^{-1} in low P soil ($P<0.05$) (Fig. 2-A). The *in situ* enzyme activities measured through zymography demonstrated a comparable pattern, being 8–28% higher for maize grown in high P soil relative to low P soil (74–100 ppmol mm^{-2} h^{-1} *vs*. 57–92 ppmol mm^{-2} h^{-1}) ($P<0.05$) (Figs. 2-C and 3). Unlike maize, the soil and *in situ* enzyme activities of lupine grown in low and high P soils remained comparable (Figs. 2-B and D and 3). The rhizosphere extent for ACP in maize and Cello in lupine grown in low P soil was 1.5 and 0.7 mm wider, respectively, than in high P soil (Fig. 2-E and F). The enzyme hotspot areas for ACP, Cello, and NAG in maize grown in high P soil were 1.8–6.5 times larger than those in low P soil, with values ranging from 82 to 535 cm^2 in high P soil compared to 35 to 249 cm^2

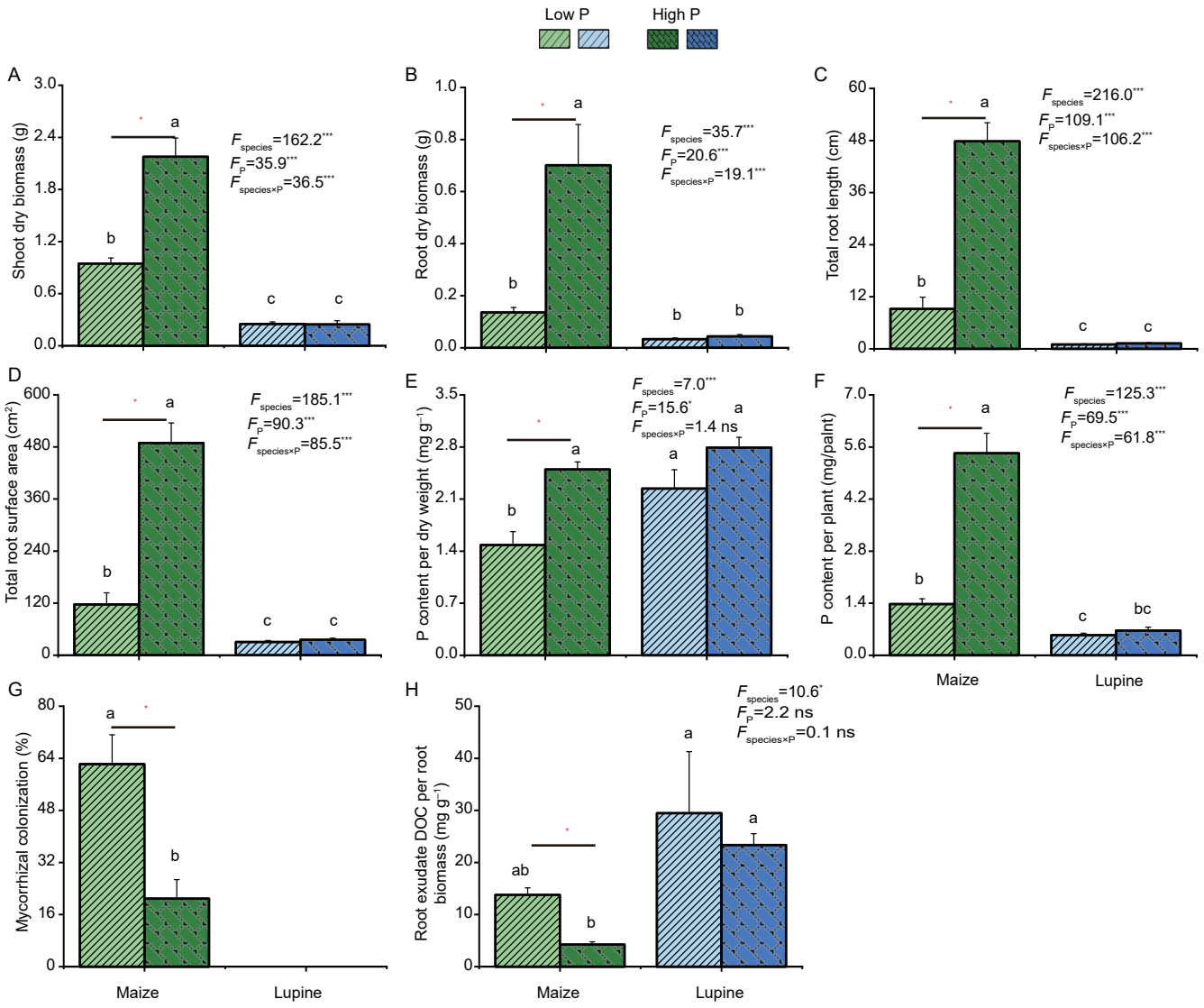


Fig. 1 Shoot dry biomass (A), root dry biomass (B), total root length (C), total root surface area (D), P content per dry weight (E), P content per plant (F), mycorrhizal colonization (G), and dissolved organic carbon (DOC) per root biomass (H) of maize and lupine cultivated under low and high phosphorus (P) concentrations in the soil. Letters denote significant differences between P supplementation and plant species following one-way ANOVA (P<0.05, Duncan's test). Red asterisk indicates significant differences between P supplementation following Student's t-test (P<0.05). Asterisks denote significant differences between plant species and P supplementation following two-way ANOVA (*, P<0.001; **, P<0.01; ***, P<0.05). Error bars represent SE (n=6).

in low P soil (P<0.05) (Fig. 2-G). Conversely, the areas of Cello hotspots for lupine grown in low P soil were 1.4–1.9 times larger than those in high P soil (186 cm^2 *vs*. 96 cm^2) (P<0.05) (Fig. 2-H).

3.3. Effects of P availability on the bacterial community composition and the bacterial co-occurrence network

High P availability enhanced bacterial community diversity (Shannon index) in the rhizospheres of both maize and lupine compared to low P (P<0.05) (Appendix B-a). Plant species and P availability significantly influenced the bacterial community structure, as revealed by principal coordinates analysis (Appendix B-b). The dominant bacterial taxa in the rhizospheres of both maize and lupine, regardless of P availability, comprised Proteobacteria (39–54%), Bacteroidota (12–21%), Actinobacteriota (5–13%), Chloroflexi (4–6%), Planctomycetota (2–5%), and Acidobacteriota (2–3%) (Appendix B-c).

For maize, Actinobacteriota, Chloroflexia, and Alphaproteobacteria (K strategists) showed enrichment in high P soil, and the numbers of gene copies encoding ACP, BG, Cello, and NAG under high P were 1.2–3.2 times greater than those under low P (P<0.05) (Fig. 4-A; Appendix C-a, b, e and f). Ktedonobacteria (r-strategist) exhibited enrichment under low P, and the numbers of gene copies encoding BG, Cello, and NAG under low P were 56–97% higher than those under high P (P<0.05) (Fig. 4-A; Appendix C-a, b, e and f).

Similarly, for lupine, Actinobacteriota (K-strategist), Bacteroidota (r strategy), and Gemmatimonadota showed enrichment in high P soil, with their gene copy numbers for BG, Cello, and NAG under high P being 1.07–5.83 times

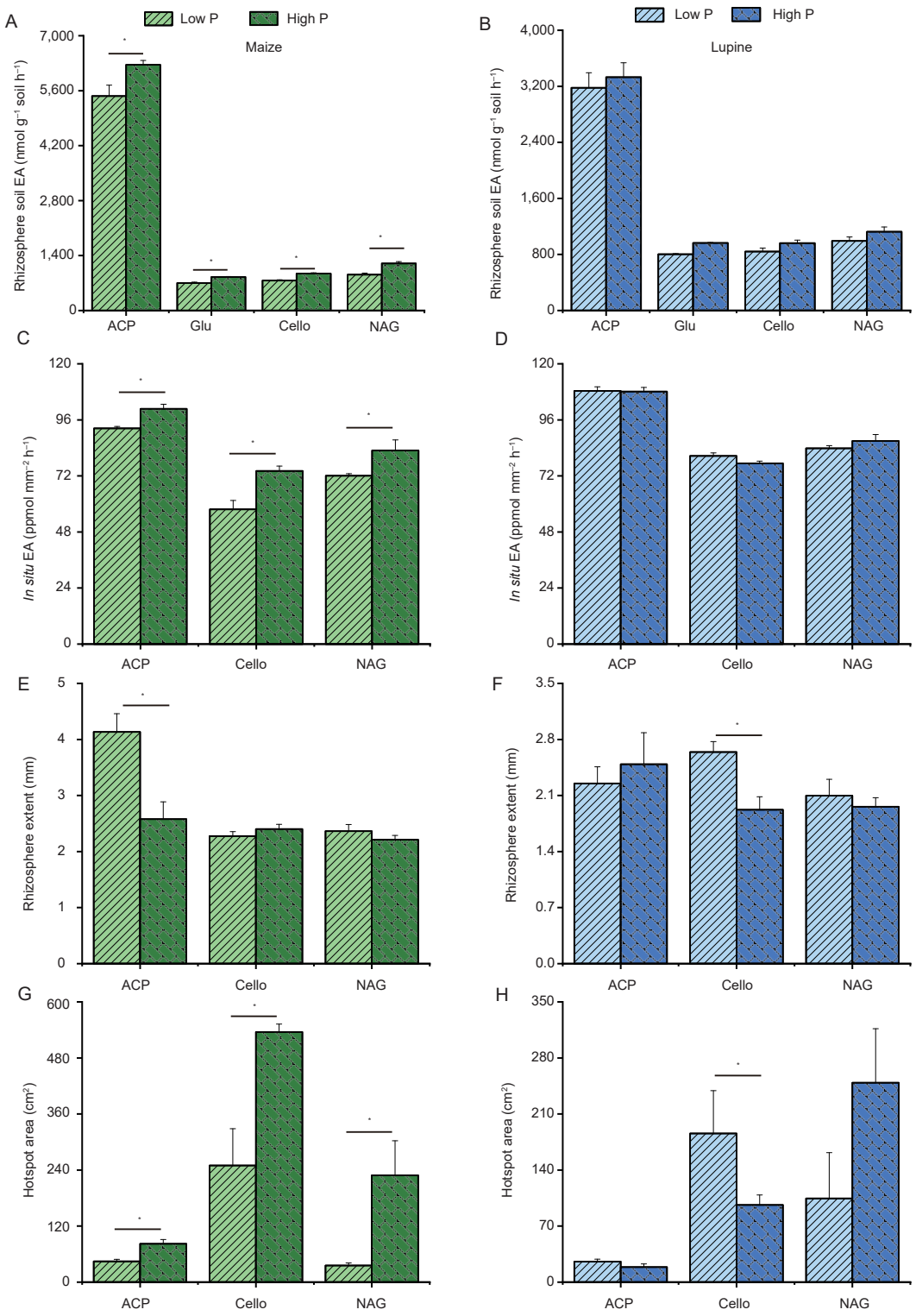


Fig. 2 Enzyme activities (EA) in the rhizosphere, *in situ* EA measured through zymography, rhizosphere extent, and hotspot areas of acid phosphatase (ACP), cellobiohydrolase (Cello) and β-N-acetylglucosaminidase (NAG) of maize (A, C, E, and G) and lupine (B, D, G and H) cultivated in soil with low and high phosphorus (P) amendments. Asterisk denote significant differences (P<0.05, Student's t-test) in response to P addition. Error bars represent SE (n=6).

greater than those under low P. Proteobacteria (r strategy) demonstrated enrichment under low P in lupine, and the number of gene copies encoding ACP under low P was 47% higher than under high P (Fig. 4-B; Appendix C-c, d, g and i).

For both maize and lupine, P availability modified the structure of the microbial network, with fewer nodes, links, and a lower links-to-nodes ratio under low P than under high P (Fig. 5). Microbial communities exhibited more positive associations in low P soil compared to high P soil (79% *vs*. 53%) for maize (Fig. 5-A and B), although this pattern

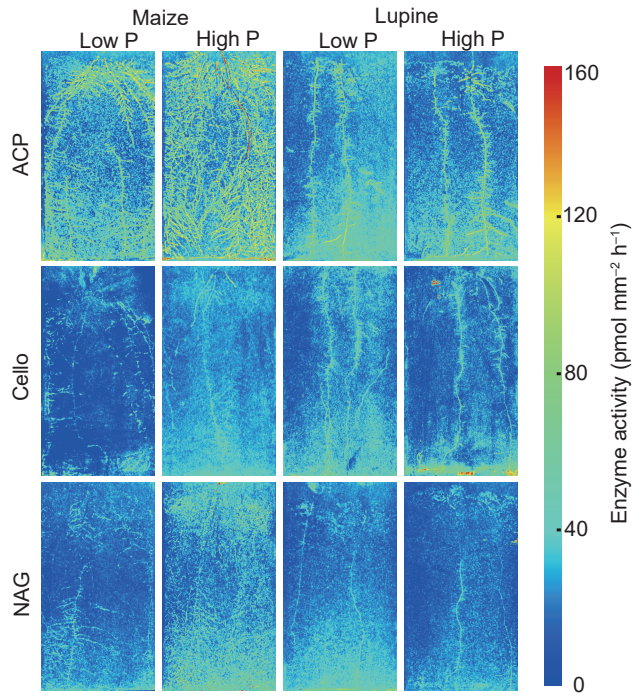


Fig. 3 Spatial distribution patterns of acid phosphatase (ACP), cellobiohydrolase (Cello), and β-N-acetylglucosaminidase (NAG) activities in maize and lupine plants grown in soils with different phosphorus (P) concentrations. The adjacent color scale represents enzyme activity measurements (pmol mm^{-2} h^{-1}).

appeared less pronounced for lupine (Fig. 5-C and D).

3.4. Linking the bacterial community composition with enzyme activities, hotspot areas, functional genes, and root exudates

The relative abundance of microorganisms identified by the LEfSe analysis demonstrated direct proportionality to the number of enzyme gene copies in the corresponding group for both lupine and maize (Fig. 6). In maize, enzyme activities and hotspot areas increased with the proportional abundance of Actinobacteriota, Chloroflexia, and Alphaproteobacteria, while decreasing with the proportional abundance of Ktedonobacteria and Xanthomonadales (Fig. 6-A). The relative abundances of Actinobacteriota and Alphaproteobacteria exhibited inverse correlation with DOC and organic acid content per root dry weight of maize (Fig. 6-A). In lupine, enzyme activities of hydrolases (Glu, Cello, and NAG) showed partial positive correlation with the abundance of Actinobacteriota, Bacteroidota, and Gemmatimonadota, while β-glucosidase activity decreased with Proteobacteria abundance (Fig. 6-B). The analysis revealed no significant correlations between the relative abundance of bacteria identified by LEfSe and hotspot areas or root exudates (DOC and organic acid content per root dry weight) for lupine (Fig. 6-B).

4. Discussion

4.1. Spatial patterns of enzyme activity in response to P availability were shaped by plant growth and the release of root exudates

Consistent with our first hypothesis, maize growth declined under low P, while lupine did not exhibit this pattern of suppression. This difference may be attributed to lupine's superior adaptation to P deficiency rather than lower P requirements compared to maize. This interpretation is supported by lupine's higher P content per dry weight than maize under low P conditions (Fig. 1-E), and lupine's organic acid release being 2–19 times greater than maize (Appendix A). Organic acids demonstrate efficiency in solubilizing complex organic P and Al/Fe oxides of P (Hocking 2001), which commonly predominate in highly weathered soils.

Maize grown in high P soil demonstrated increased shoot and root biomass, enhanced root length, and greater root surface area, facilitating enzyme hotspot formation (Figs. 1-C and D, and 2-G). However, root-released C and carboxylate per unit of dry weight decreased with increasing

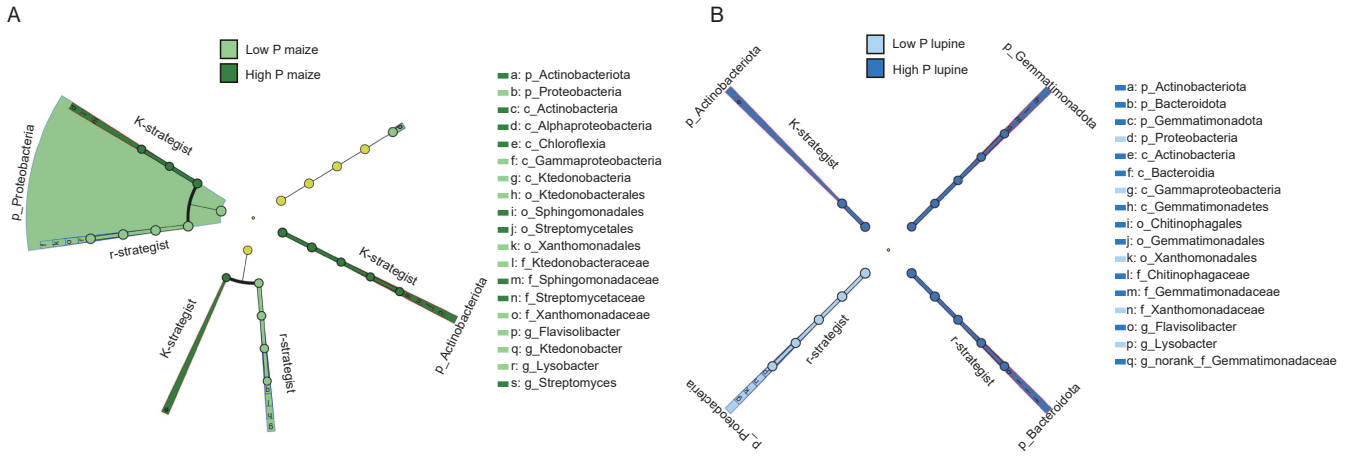


Fig. 4 LEfSe illustrates the significantly abundant bacterial taxa in response to phosphorus (P) supplementation in the rhizosphere of maize (A) and lupine (B). The concentric circles, arranged from exterior to interior, represent taxonomic levels from phylum to genus. Individual circles denote specific classifications at each level. Green and blue color nodes indicate taxa significantly enriched in their respective groups, while yellow color nodes represent taxa showing no significant differentiation.

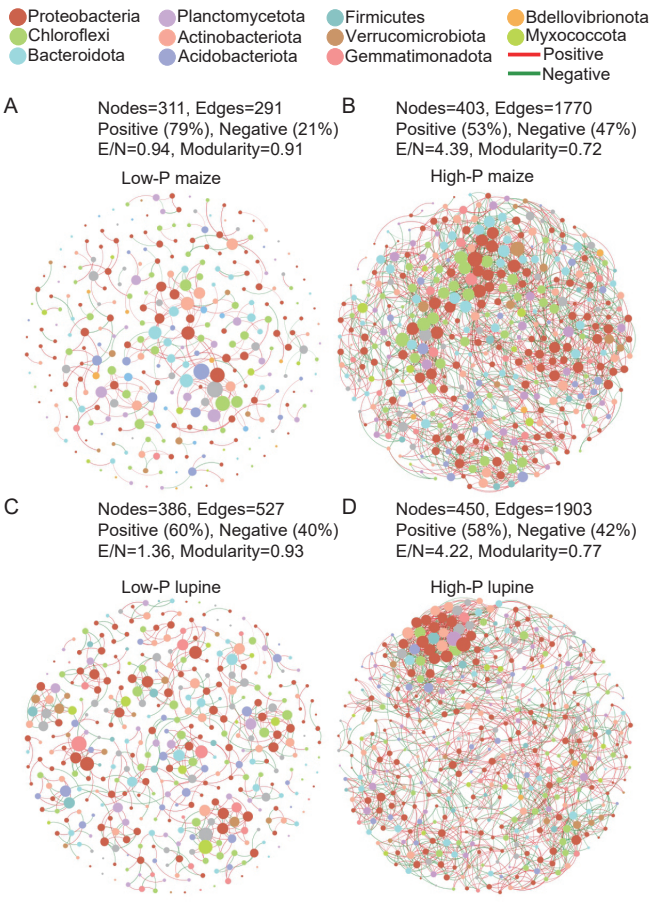


Fig. 5 Co-occurrence network analysis revealing the bacterial community structures in the rhizosphere of maize and lupine grown in soils with low and high phosphorus (P) availability. The network displays connections between nodes representing Spearman's r>0.8 and statistically significant (P<0.05) correlations. Nodes are differentiated by color according to bacterial phyla, providing a visual representation of community composition and illustrating significant interactions within the microbial network. E/N indicates edges divide nodes.

P content (Fig. 1-H; Appendix A). Consequently, rhizosphere microorganisms under high P treatment experienced C limitation, necessitating increased enzyme synthesis and release for organic matter hydrolysis. This was evidenced by 8–31% higher activities of Glu, Cello, and NAG in maize grown in high P soil compared to low P soil (Fig. 2-A and C).

Contrary to expectations, ACP activity in the rhizosphere soil and *in situ* activity for maize under high P exceeded that in low P soil. This observation can be attributed to the increased proportion of K-strategists under high P conditions (Fig. 4-A), as K-strategists demonstrate higher ACP production efficiency (Leff *et al.* 2015; Roller and Schmidt 2015). Despite lower ACP activity under low P, the rhizosphere extent was 1.5 mm greater than under high P. This suggests maize's implementation of alternative strategies, including root morphological changes and enhanced mycorrhizal colonization, for Pi acquisition (Ma *et al.* 2021c). Specifically, minor increases in root hair length and enhanced mycorrhizal fungi colonization (Ma *et al.* 2021b; Wen *et al.* 2019) expand the rhizosphere extent (Fig. 1-H). Additionally, increased root exudates (DOC and organic acid) (Fig. 1-H) can diffuse further from the root surface, expanding the rhizosphere (Lambers *et al.* 2015). Expanding the ACP activity rhizosphere area serves as an effective mechanism for plants to obtain Pi from larger soil volumes (Ma *et al.* 2018), mitigating nutrient competition between rhizosphere microorganisms and roots (Kuzyakov and Xu 2013).

Given its robust adaptation to P deficiency, lupine did not exhibit differences in enzyme activities and hotspot areas in response to P availability, as initially hypothesized. However, lupine demonstrated a broader rhizosphere and larger hotspot areas of Cello activity under low P conditions (Fig. 2-F and H). This resulted from slightly higher DOC and carboxylate release (Fig. 1-H; Appendix A), promoting microbial growth and enzyme production. Thus, rhizosphere C and P cycling demonstrate interconnection, as P availability influences plant growth, root exudate release, and nutrient acquisition strategies, which subsequently impact C cycling enzyme activities, enzyme hotspots, and rhizosphere extent.

4.2. Phosphorus availability affects the bacterial community and network

Limited P availability reduced bacterial diversity compared to high P conditions (Appendix B). This reduction can be attributed to enhanced root exudate release per unit root biomass under P-limited conditions (Fig. 1-H; Appendix A). Certain fast-growing bacteria (i.e., r-strategists) utilize these exudates efficiently, thereby inhibiting the growth of other microbial species (Mau *et al.* 2015). This observation is supported by the increased presence of r-strategists such as Gammaproteobacteria, Xanthomonadales, and Flavisolibacter under low P conditions, while K-strategists including Actinobacteriota, Chloroflexia, and Alphaproteobacteria showed higher abundance under high P conditions in maize (Fig. 4-A). These patterns demonstrate greater prominence in the rhizosphere, where substrate availability exceeds that of bulk soil (Ling *et al.* 2022).

Phosphorus availability significantly influenced microbial interactions beyond bacterial community composition. Under low P conditions, the bacterial network exhibited reduced nodes, links, and a lower links-to-nodes ratio compared to high P conditions (Fig. 5), indicating simplified bacterial co-occurrence networks (Zhang *et al.* 2024). Despite this structural simplification, maize rhizosphere bacterial communities demonstrated increased positive correlations under low P conditions (Fig. 5-A), suggesting enhanced microbial cooperation (Sasse *et al.* 2018). Although cooperative interactions may enhance microbial P acquisition during deficiency, they intensify competition with plant roots, which compromising plant growth over time (Kuzyakov and Xu 2013).

In lupine, both Actinobacteriota (K-strategists) and Bacteroidota (r-strategists) showed enrichment under high P conditions, suggesting no distinct shift in bacterial community composition between contrasting nutrient-use strategists (Fig. 4-B). Furthermore, the distribution of positive

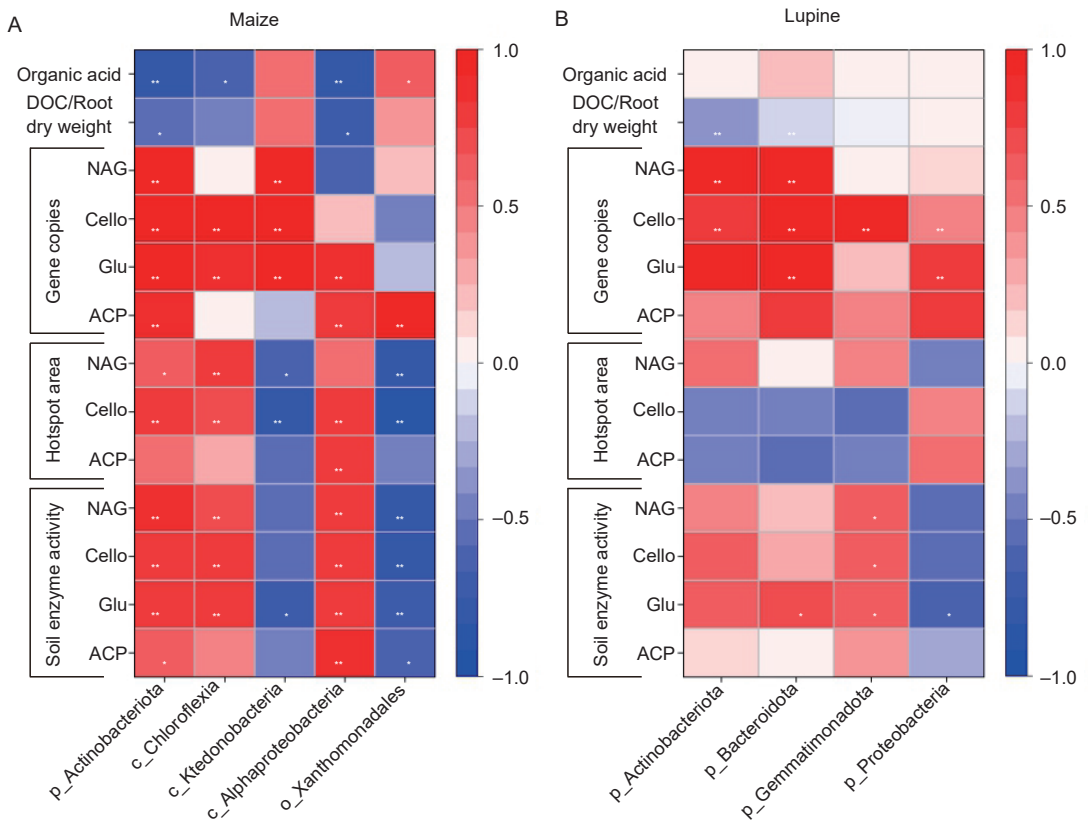


Fig. 6 Heatmap depicting Spearman correlations between the relative abundances of microbial taxonomic groups identified through LEfSe analysis and soil parameters including enzyme activity, hotspot area, enzyme gene copies, and DOC/root dry weight. ACP, Glu, Cello and NAG represent acid phosphatase, β-glucosidase, cellobiohydrolase (Cello) and β-N-acetylglucosaminidase (NAG), respectively. * and ** indicate significant correlations at $P<0.05$ and $P<0.01$, respectively.

and negative microbial associations in bacterial networks remained consistent between low and high P conditions (Fig. 5-C and D). This stability corresponds to lupine's limited response to P availability regarding growth and root exudate release (Fig. 1-B and H; Appendix A). These findings demonstrate how plant adaptability to P deficiency influences plant growth and root exudate production, subsequently affecting rhizosphere bacterial community composition and connectivity.

4.3. Relationships between the bacterial community and enzyme activities, the rhizosphere gene copies and enzyme hotspots

The relative abundances of bacterial taxa identified through LEfSe analysis demonstrated direct proportionality to enzyme gene copy numbers in their respective microbial groups. Given that functional gene copies frequently indicate microbial community abundance (Trivedi *et al.* 2016; Ma *et al.* 2023), this relationship establishes a clear connection between bacterial composition and enzyme production. In maize, soil enzyme activity and enzyme hotspot areas increased with K-strategist abundance (Actinobacteriota, Chloroflexia, and Alphaproteobacteria) but decreased with r-strategists (Ktedonobacteria and Xanthomonadales) (Fig. 6-A). K-strategists demonstrate superior C allocation efficiency, directing resources toward enzyme synthesis rather than respiration (Fang *et al.* 2018; Wang X *et al.* 2021; Bian *et al.* 2022). Consequently, enhanced enzyme activities and expanded hotspot areas in the maize rhizosphere under high P conditions correlated with increased root system size (Fig. 1-A and C) and microbial community transition toward K-strategists, which optimize resource allocation for enzyme synthesis (Fig. 7).

For lupine, however, bacterial abundance identified through LEfSe analysis showed no significant impact on enzyme hotspot areas and only partial correlation with enzyme activity (Fig. 6-B). This indicates that bacterial community changes in response to P availability exhibited less influence on enzyme activity spatial distribution in lupine rhizosphere compared to maize. These results demonstrate that plant adaptability to P deficiency shapes both rhizosphere bacterial communities and enzyme activity spatial organization, with maize showing stronger bacterial-enzyme interactions than lupine. Future research should examine a wider range of plant species with diverse P adaptation and acquisition strategies to determine the universality of these phenomena.

5. Conclusion

This investigation utilized zymography combined with high-throughput sequencing to examine how P availability affects plant growth, root morphology and physiology, bacterial community structure and function, and enzyme activity

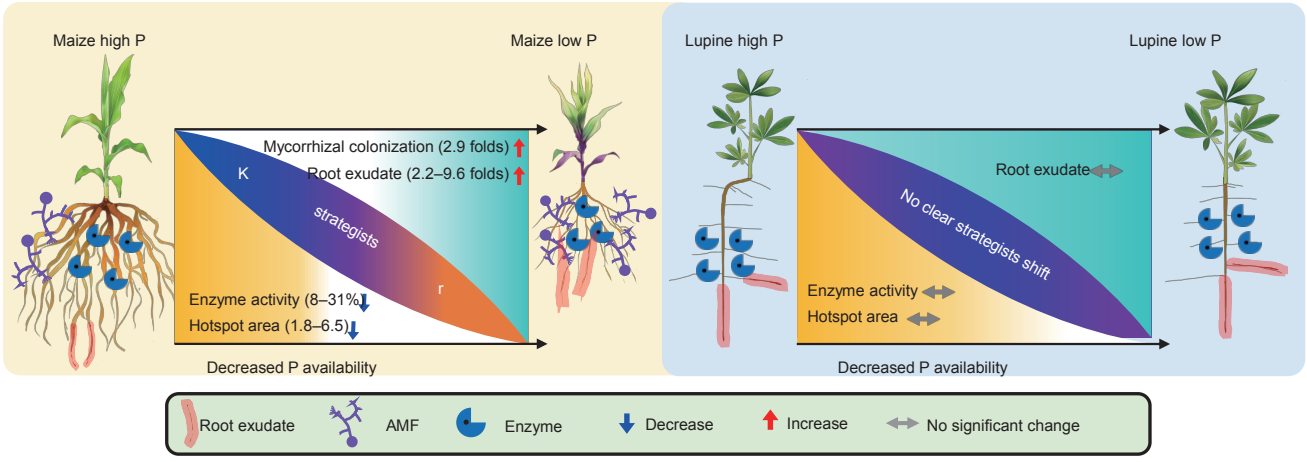


Fig. 7 Schematic representation illustrating the adaptive mechanisms and acquisition strategies for phosphorus (P) deficiency that influence enzyme activity distribution in the rhizosphere and bacterial community composition of maize and lupine. Red and blue arrows adjacent to the numbers indicate increases and decreases in the respective variables in response to phosphorus availability. Grey double arrows indicate no significant change. AMF stands for arbuscular mycorrhizal fungi.

spatial distribution in the rhizospheres of maize and lupine — species with distinct P deficiency adaptation strategies. The results demonstrate strong coupling between C and P cycling in the rhizosphere, mediated by plant–microbe interactions. P availability influenced not only plant growth and root-derived C-cycle enzyme production but also C allocation to belowground biomass, subsequently affecting bacterial community composition, functional traits, and spatial enzyme activity patterns. Maize demonstrated greater P deficiency sensitivity, exhibiting pronounced responses in growth and root exudation compared to lupine. This resulted in significant changes in C-cycle-related enzyme activity spatial organization and substantial shifts in bacterial community structure and function. These findings establish P availability as a crucial factor in determining rhizosphere C-cycling enzyme activity spatial distribution, mediated through plant–microbe interactions and plant P deficiency adaptability.

Acknowledgements

This study was supported by the National Key R&D Program of China (2023YFD1901800), the National Natural Science Foundation of China (32371726, 42307421 and 42407449), and the Peoples Friendship University of Russia (RUDN University) Strategic Academic Leadership Program, Russia.

Declaration of competing interest

The authors declare that they have no conflict of interest.

Declaration of generative AI and AI-assisted technologies in the writing process

The authors declare that they did not use AI in the preparation and writing of this manuscript.

Appendices associated with this paper are available at https://doi.org/10.1016/j.jia.2025.08.017

References

Bardgett R D, Mommer L, De Vries F T. 2014. Going underground: Root traits as drivers of ecosystem processes. *Trends in Ecology & Evolution*, **29**, 692–699.

Bastian M, Heymann S, Jacomy M. 2009. Gephi: An open source software for exploring and manipulating networks visualization and exploration of large graphs. *Proceedings of the International AAAI Conference on Web and Social Media*, **3**, 361–362.

Bian Q, Wang X, Bao X, Che Z, Sun B, Zhu L, Xie Z. 2022. Exogenous substrate quality determines the dominant keystone taxa linked to carbon mineralization: Evidence from a 30-year experiment. *Soil Biology & Biochemistry*, **169**, 108683.

Chen Q, Zhao Q, Xie B, Lu X, Guo Q, Liu G, Zhou M, Tian J, Lu W, Chen K, Tian J, Liang C. 2024. Soybean (*Glycine max*) rhizosphere organic phosphorus recycling relies on acid phosphatase activity and specific phosphorus-mineralizing-related bacteria in phosphate deficient acidic soils. *Journal of Integrative Agriculture*, **23**, 1685–1702.

Choreño-Parra E M, Treseder K K. 2024. Mycorrhizal fungi modify decomposition: A meta-analysis. *New Phytologist*, **242**, 2763–2774.

Cong W, Suriyagoda L D B, Lambers H. 2020. Tightening the phosphorus cycle through phosphorus-efficient crop genotypes. *Trends in Plant Science*, **25**, 967–975.

Edgar R C. 2013. UPARSE: Highly accurate OTU sequences from microbial amplicon reads. *Nature Methods*, **10**, 996–998.

Fang Y, Nazaries L, Singh B K, Singh B P. 2018. Microbial mechanisms of carbon priming effects revealed during the interaction of crop residue and nutrient inputs in contrasting soils. *Global Change Biology*, **24**, 2775–2790.

Faust K, Raes J. 2012. Microbial interactions: From networks to models. *Nature Reviews Microbiology*, **10**, 538–550.

Frey S D. 2019. Mycorrhizal fungi as mediators of soil organic matter dynamics. *Annual Review of Ecology, Evolution, and Systematics*, **50**, 237–259.

Hammond J P, White P J. 2008. Sucrose transport in the phloem: Integrating root responses to phosphorus starvation. *Journal of Experimental Botany*, **59**, 93–109.

Hao C, Dungait J A J, Wei, X, Ge T, Kuzyakov Y, Cui Z, Tian J, Zhang F. 2022. Maize root exudate composition alters rhizosphere bacterial community to control hotspots of hydrolase activity in response to nitrogen supply. *Soil Biology & Biochemistry*, **170**, 108717.

Hinsinger P. 2001. Bioavailability of soil inorganic P in the rhizosphere as affected by root-induced chemical changes: A review. *Plant and Soil*, **237**, 173–195.

Hocking P J. 2001. Organic acids exuded from roots in phosphorus uptake and aluminum tolerance of plants in acid soils. *Agronomy*, **74**, 63–97.

Jiang Z, Vancov T, Fang Y, Tang C, Zhang W, Xiao M, Song X, Zhou J, Ge T, Cai Y, Yu B, White J C, Li Y. 2025. Sustained superiority of biochar over straw for enhancing soil biological-phosphorus via the mediation of *phoD*-harboring bacteria in subtropical Moso bamboo forest. *Forest Ecology and Management*, **584**, 122606.

Kuzyakov Y, Xu X. 2013. Competition between roots and microorganisms for nitrogen: Mechanisms and ecological relevance. *New Phytologist*, **198**, 656–669.

Lambers H. 2022. Phosphorus acquisition and utilization in plants. *Annual Review of Plant Biology*, **73**, 1–26.

Lambers H, Finnegan P M, Jost R, Plaxton W C, Shane M W, Stitt M. 2015. Phosphorus nutrition in Proteaceae and beyond. *Nature Plants*, **1**, 1–9.

Leff J W, Jones S E, Prober S M, Barberán A, Borer E T, Firn J L, Harpole W S, Hobbie S E, Hofmockel K S, Knops J M H, McCulley R L, La Pierre K, Risch A C, Seabloom E W, Schütz M, Steenbock C, Stevens C J, Fierer N. 2015. Consistent responses of soil microbial communities to elevated nutrient inputs in grasslands across the globe. *Proceedings of the National Academy of Sciences of the United States of America*, **112**, 10967–10972.

Li Z, Duan X, Guo X, Gao W, Li Y, Zhou P, Zhu Q, O'Donnell A G, Dai K, Wu J. 2024. Microbial metabolic capacity regulates the accrual of mineral-associated organic carbon in subtropical paddy soils. *Soil Biology & Biochemistry*, **195**, 109457.

Ling N, Wang T, Kuzyakov Y. 2022. Rhizosphere bacteriome structure and functions. *Nature Communications*, **13**, 1–13.

Ma X, Geng Q, Zhang H, Bian C, Chen H Y H, Jiang D, Xu X. 2021a. Global negative effects of nutrient enrichment on arbuscular mycorrhizal fungi, plant diversity and ecosystem multifunctionality. *New Phytologist*, **229**, 2957–2969.

Ma X, Li X, Ludewig U. 2021b. Arbuscular mycorrhizal colonization outcompetes root hairs in maize under low phosphorus availability. *Annals of Botany*, **127**, 155–166.

Ma X, Liu Y, Shen W, Kuzyakov Y. 2021c. Phosphatase activity and acidification in lupine and maize rhizosphere depend on phosphorus availability and root properties: Coupling zymography with planar optodes. *Applied Soil Ecology*, **167**, 104029.

Ma X, Liu Y, Zarebanadkouki M, Razavi B S, Blagodatskaya E, Kuzyakov Y. 2018. Spatiotemporal patterns of enzyme activities in the rhizosphere: Effects of plant growth and root morphology. *Biology and Fertility of Soils*, **54**, 819–828.

Ma X, Mason-Jones K, Liu Y, Blagodatskaya E, Kuzyakov Y, Guber A, Dippold M A, Razavi B S. 2019. Coupling zymography with pH mapping reveals a shift in lupine phosphorus acquisition strategy driven by cluster roots. *Soil Biology & Biochemistry*, **135**, 420–428.

Ma X, Zhou Z, Chen J, Xu H, Ma S, Dippold M A, Kuzyakov Y. 2023. Long-term nitrogen and phosphorus fertilization reveals that phosphorus limitation shapes the microbial community composition and functions in tropical montane forest soil. *Science of the Total Environment*, **854**, 158709.

Ma X, Zhu B, Nie Y, Liu Y, Kuzyakov Y. 2021d. Root and mycorrhizal strategies for nutrient acquisition in forests under nitrogen deposition: A meta-analysis. *Soil Biology & Biochemistry*, **163**, 108418.

Mau R L, Liu C M, Aziz M, Schwartz E, Dijkstra P, Marks J C, Price L B, Keim P, Hungate B A. 2015. Linking soil bacterial biodiversity and soil carbon stability. *The ISME Journal*, **9**, 1477–1480.

Neumann G, Martinoia E. 2002. Cluster roots — An underground adaptation for survival in extreme environments. *Trends in Plant Science*, **7**, 162–167.

Pang J, Bansal R, Zhao H, Bohuon E, Lambers H, Ryan M H, Ranathunge K, Siddique K H M. 2018. The carboxylate-releasing phosphorus-mobilizing strategy can be proxied by foliar manganese concentration in a large set of chickpea germplasm under low phosphorus supply. *New Phytologist*, **219**, 518–529.

Parihar M, Rakshit A, Meena V S, Gupta V K, Rana K, Choudhary M, Tiwari G, Mishra P K, Pattanayak A, Bisht J K, Jatav S S, Khati P, Jatav H S. 2020. The potential of arbuscular mycorrhizal fungi in C cycling: A review. *Archives of Microbiology*, **202**, 1581–1596.

Philippot L, Raaijmakers J M, Lemanceau P, Van Der Putten W H. 2013. Going back to the roots: The microbial ecology of the rhizosphere. *Nature Reviews Microbiology*, **11**, 789–799.

Postma J A, Dathe A, Lynch J P. 2014. The optimal lateral root branching density for maize depends on nitrogen and phosphorus availability. *Plant Physiology*, **166**, 590–602.

Roller B R K, Schmidt T M. 2015. The physiology and ecological implications of efficient growth. *The ISME Journal*, **9**, 1481–1487.

Sasse J, Martinoia E, Northen T. 2018. Feed your friends: Do plant exudates shape the root microbiome? *Trends in Plant Science*, **23**, 25–41.

Segata N, Izard J, Waldron L, Gevers D, Miropolsky L, Garrett W S, Huttenhower C. 2011. Metagenomic biomarker discovery and explanation. *Genome Biology*, **12**, R60.

Shang W, Razavi B.S, Yao S, Hao C, Kuzyakov Y, Blagodatskaya E, Tian J. 2023. Contrasting mechanisms of nutrient mobilization in rhizosphere hotspots driven by straw and biochar amendment. *Soil Biology & Biochemistry*, **187**, 109212.

Soong J L, Marañon-jimenez S, Cotrufo M F, Boeckx P, Bodé S, Guenet B, Peñuelas J, Richter A, Stahl C, Verbruggen E, Janssens I A. 2018. Soil microbial CNP and respiration responses to organic matter and nutrient additions : Evidence from a tropical soil incubation. *Soil Biology & Biochemistry*, **122**, 141–149.

Trivedi P, Delgado-Baquerizo M, Trivedi C, Hu H, Anderson I C, Jeffries T C, Zhou J, Singh B K. 2016. Microbial regulation of the soil carbon cycle: Evidence from gene-enzyme relationships. *The ISME Journal*, **10**, 2593–2604.

Trouvelot A, Kough J L, Gianinazzi-Pearson V. 1986. Mesure du taux de mycorhization VA d'un système radiculaire. Recherche de méthodes d'estimation ayant une signification fonctionnelle. In: Pearson G, Gianinazzi S, eds., *Physiological and Genetical Aspects of Mycorrhizae*. *Proceedings of the 1st European Symposiurn on Mycorrhizae*. Institut National de la Recherche Agronomiqu, Paris. pp. 217–221. (in French)

Vierheilig H, Coughlan A P, Wyss U, Piché Y. 1998. Ink and vinegar, a simple staining technique for arbuscular-mycorrhizal fungi. *Applied and Environmental Microbiology*, **64**, 5004–5007.

Walker T S, Bais H P, Grotewold E, Vivanco J M. 2003. Root exudation and rhizosphere biology *Plant Physiology*, **132**, 44–51.

Wang C, Kuzyakov Y. 2024. Rhizosphere engineering for soil carbon sequestration. *Trends in Plant Science*, **29**, 447–468.

Wang L, Li X, Mang M, Ludewig U, Shen J. 2021. Heterogeneous nutrient supply promotes maize growth and phosphorus acquisition : Additive and compensatory effects of lateral roots and root hairs. *Annals of Botany*, **128**, 431–440.

Wang X, Zhang W, Liu Y, Jia Z, Li H, Yang Y, Wang D, He H, Zhang X. 2021. Identification of microbial strategies for labile substrate utilization at phylogenetic classification using a microcosm approach. *Soil Biology & Biochemistry*, **153**, 107970.

Wen Z, Li H, Shen Q, Tang X, Xiong C, Li H, Pang J, Ryan M H, Lambers H, Shen J. 2019. Tradeoffs among root morphology, exudation and mycorrhizal symbioses for phosphorus-acquisition strategies of 16 crop species. *New Phytologist*, **223**, 882–895.

WRB (World Reference Base for Soil Resources). 2006. *A Framework for International Classification*, *Correlation and Communication*. Food and Agriculture Organization of the United Nations, Rome.

Zhang D, Zhang C, Tang X, Li H, Zhang F, Rengel Z, Whalley W R, Davies W J, Shen J. 2016. Increased soil phosphorus availability induced by faba bean root exudation stimulates root growth and phosphorus uptake in neighbouring maize. *New Phytologist*, **209**, 823–831.

Zhang T, Liu Y, Ge S, Peng P, Tang H, Wang J. 2024. Sugarcane/soybean intercropping with reduced nitrogen addition enhances residue-derived labile soil organic carbon and microbial network complexity in the soil during straw decomposition. *Journal of Integrative Agriculture*, **23**, 4216–4236.

Zhang X, Myrold D D, Shi L, Kuzyakov Y, Dai H, Thu Hoang D T, Dippold M A, Meng X, Song X, Li Z, Zhou J, Razavi B S. 2021. Resistance of microbial community and its functional sensitivity in the rhizosphere hotspots to drought. *Soil Biology & Biochemistry*, **161**, 108360.

Executive Editor-in-Chief Keke Yi
Managing Editor Lujuan Sun